Published in Journal of Electroanalytical Chemistry 614, issues 1-2, 15-23, 2008
which should be used for any reference to this work

Theory and computer simulation of the time-dependent selectivity behavior of polymeric membrane ion-selective electrodes

W.E. Morf [a,*], E. Pretsch [b], N.F. de Rooij [a]

[a] *Institute of Microtechnology, University of Neuchâtel, Rue Jaquet-Droz 1, CH-2007 Neuchâtel, Switzerland*
[b] *Laboratory of Organic Chemistry, ETH Zurich, CH-8093 Zurich, Switzerland*

Abstract

A theoretical treatment of the time-dependent potential response of ion-selective electrodes to sample solutions containing primary and interfering ions is presented. The theory accounts for the influence of ion fluxes in the electrode membrane and the contacting aqueous sample layer and describes the variations in the apparent selectivity behavior as a function of the measuring time. The applicability of the theory is demonstrated by comparing predicted response curves with results of virtual experiments based on computer simulation. A close and convincing agreement was achieved for a large series of different examples, which confirms that the new theory can be successfully applied for general cases.

Keywords: Ion-selective electrodes; Selectivity; Time-dependent response; Theory; Computer simulation; Finite-difference method

1. Introduction

For conventional polymeric membrane ion-selective electrodes (ISEs) time-dependent processes in the membrane phase are negligible when the electrodes are used in samples containing only the primary ions at concentrations above 10^{-6} M. A prerequisite is that the membrane has been preconditioned with primary ions on the sample side, and that the inner solution contains the same ions at a sufficiently high concentration [1]. Transmembrane ion fluxes are, however, highly relevant at lower sample concentrations, especially in the presence of interfering ions [2–5]. The recent spectacular improvement of the lower detection limit of ISEs by orders of magnitude relies on the reduction of such fluxes [6,7]. Measurements of sample concentrations in the sub-micromolar range require a careful design of the membrane, the inner solution, and the conditioning procedure [8]. Since ion flux effects can be massively reduced but never fully eliminated, time-dependent responses may become a limiting factor in trace determinations with potentiometric sensors.

In the absence of ion fluxes, the response of ISEs to mixed solutions of primary and interfering ions could be exactly predicted on the basis of unbiased (i.e., thermodynamic) selectivity coefficients that are related to the respective ion-exchange equilibria [9,10]. This implies that the measurements would be performed under idealized conditions at which the electrode exhibits a Nicolsky-type response to the involved ions [10]. In usual ISE practice, however, the observed selectivity behavior often deviates from the equilibrium characteristics, which indicates that diffusion-controlled kinetic influences come into play.

More recently, various ISE applications have emerged that specifically rely on transmembrane ion fluxes. For instance, sensors for polyions such as heparin or protamine are based on a counter-transport mechanism, in which the polyion of interest is depleted locally at the membrane surface during the accumulation process [11]. Since the response of these ISEs depends on the mass transport of

* Corresponding author.
E-mail address: Werner.Morf@unine.ch (W.E. Morf).

the polyion to the membrane surface, the resulting slopes of the calibration curves are significantly larger than those predicted from the Nernst equation. Other examples of non-equilibrium potentiometry include so-called steptrodes [12,13], which have an unusually high sensitivity and no need for reference devices, as well as the monitoring of chemical titrations with sensors that show larger potential changes at the endpoint than would be expected from thermodynamic considerations [14]. Recently, it was demonstrated that ISEs with thin liquid membranes allow it to calibrate from inside without altering the sample solution in any way [15,16]. Zero-current fluxes in either direction are eliminated almost instantly when the membrane-internal concentration gradient is reduced to zero by the proper choice of the composition of the inner solution.

In recent years, this area of research has been further extended to ISEs that are exposed to an external current which induces an instrumentally controlled ion flux across the membrane [17–19]. Initial examples of this technique made use of an applied current to lower the detection limit [17,18]. More recent attempts utilized larger current densities in a multi-pulse sequence to make many of the above-mentioned sensing principles fully reversible and therefore more useful for analytical measurements [13,20].

It has been shown in a series of theoretical studies that the ion selectivity behavior of ISEs may change drastically under the influence of transmembrane ion fluxes in zero-current [3–5,21] or controlled-current experiments [19]. However, these treatments were usually restricted to steady-state conditions for the mass transport in the membrane phase. Hence, the results of these approaches may be less suited for treating time-dependent response phenomena. A recent extended theory based on a combined Nernst–Planck–Poisson model for the ion fluxes is indeed capable of describing the time-dependent behavior of ISEs [22]. On the other hand, it requires a very complex numerical procedure to calculate the respective response data.

In this work, a theoretical analysis of the time-dependent ion-flux-controlled potential response of ISEs to primary and interfering ions at zero current is presented. The treatment is based on an approximate, but generally useful, description of mass fluxes in the membrane. Accordingly, the results are obtained in a relatively closed form. To document the applicability of the new theory, the predicted time-dependent responses are compared with results of virtual experiments performed by computer simulation. Details on the numerical simulation of ISEs by a finite-difference procedure have been reported in a recent contribution [23].

2. Theory

When separate-solution measurements are performed with ISEs to determine selectivity coefficients, the response to primary ions i and to interfering ions j is usually evaluated from Eqs. (1) and (2), respectively [1,9,24]:

$$E = E_i^0 + \frac{RT}{z_i F} \ln a_{i,\mathrm{aq}} \tag{1}$$

$$E = E_i^0 + \frac{RT}{z_i F} \ln K_{ij} \left(a_{j,\mathrm{aq}}\right)^{z_i/z_j} \tag{2}$$

where E is the emf, E_i^0 is the reference potential, $a_{i,\mathrm{aq}}$ and $a_{j,\mathrm{aq}}$ are the bulk activities of the respective sample solutions, z_i and z_j are the ion charges (taken here as positive), K_{ij} is the selectivity coefficient, and RT/F is the Nernst factor. It is well known that these expressions are theoretically justified only if an equilibrium state is reached in both experiments [1,9,24]. This implies that the whole system exclusively contains either ions i or j as sensed ions. In this case, K_{ij} is identical to the thermodynamically defined selectivity coefficient. In reality the experiments do often not fulfill the required equilibrium conditions, however, since two or even more different species are involved in the selectivity measurements. Accordingly, the experimentally determined selectivity coefficients, K_{ij}^{pot} [10,25], may deviate from the thermodynamic coefficients K_{ij}. It is therefore adequate to replace the above idealized expressions by the following mixed-potential approach which is based on the phase-boundary potential model [4,9,24]:

$$E = E_i^0 + \frac{RT}{z_i F} \ln \frac{a'_{i,\mathrm{aq}}}{x'_{i,\mathrm{m}}} \tag{3a}$$

$$E = E_i^0 + \frac{RT}{z_i F} \ln K_{ij} \left(\frac{a'_{j,\mathrm{aq}}}{x'_{j,\mathrm{m}}}\right)^{z_i/z_j} \tag{3b}$$

$$x'_{k,\mathrm{m}} = z_k \frac{C'_{k,\mathrm{m}}}{R_{\mathrm{tot}}}, \quad \sum_k x'_{k,\mathrm{m}} = 1 \tag{4, 5}$$

where $a'_{k,\mathrm{aq}}$ is the activity of ions k (i or j) in the sample boundary next to the electrode, $C'_{k,\mathrm{m}}$ is the concentration of the ions (either free or as complexes) on the membrane surface, R_{tot} is the total concentration of ionic sites r (here trapped anions) in the membrane, and $x'_{k,\mathrm{m}}$ is the local molar fraction of sites occupied by ions k. In Eq. (3) K_{ij} corresponds to the thermodynamic selectivity coefficient because a local equilibrium is usually established at the interface due to fast ion-exchange kinetics. On the other hand, deviations between bulk and boundary sample activities as well as variations in the membrane composition still give rise to distinct phenomena of non-equilibrium responses.

If the ISE membrane has been freshly prepared and symmetrically conditioned with a given ionic composition, it contains uniform initial concentrations $C_{k,\mathrm{m}}^0$ (or molar fractions $x_{k,\mathrm{m}}^0$) of exchangeable ions k. This implies that, prior to the actual measurement, the membrane is exposed on the sample side to a solution that has exactly the same composition as the inner solution. A general treatment of the time-dependent potential response based on finite difference in time and finite element in space is available in the literature [26]. An extension of the present approach for asymmetrical preconditioning modes is given in the

Appendix. A sample change at the time $t = 0$ then induces concentration changes from $C^0_{k,\mathrm{m}}$ to $C'_{k,\mathrm{m}}$ at the interface. The resulting ion diffusion into the membrane can be approximated by [4,27]

$$J_k = \frac{D_\mathrm{m}}{\delta_\mathrm{m}(t)}\left(C'_{k,\mathrm{m}} - C^0_{k,\mathrm{m}}\right) = \frac{D_\mathrm{m}}{\delta_\mathrm{m}(t)}\left(x'_{k,\mathrm{m}} - x^0_{k,\mathrm{m}}\right)R_\mathrm{tot}/z_k \qquad (6)$$

$$\delta_\mathrm{m}(t) = \sqrt{\kappa D_\mathrm{m} t} \qquad (7)$$

$$x^0_{k,\mathrm{m}} = z_k\frac{C^0_{k,\mathrm{m}}}{R_\mathrm{tot}}, \quad \sum_k x^0_{k,\mathrm{m}} = 1 \qquad (8,9)$$

where J_k is the flux of ions k from the interface, D_m is the diffusion coefficient in the membrane, assumed to be the same for all ions k, δ_m is the time-dependent thickness of the diffusion layer formed in the membrane, and κ is a numerical factor that ranges between the limits π and $4/\pi$ and is averaged by the value 2 (see Appendix). Obviously, δ_m must be smaller than the total membrane thickness that becomes decisive in steady-state descriptions [4]. It should be noted that Eqs. (6)–(9) fulfill the condition for zero current, $\sum_k z_k J_k = 0$.

The diffusion processes in the membrane phase are coupled to ion fluxes through the stagnant diffusion layer of the sample solution, which is related to the hydrodynamically controlled boundary layer [28–30]. Since diffusion in the aqueous phase is much faster than in the membrane, the steady-state assumption can be used to describe the flux of ions k through the aqueous boundary film

$$J_k = \frac{D_{k,\mathrm{aq}}}{\gamma_{k,\mathrm{aq}}\delta_\mathrm{aq}}\left(a_{k,\mathrm{aq}} - a'_{k,\mathrm{aq}}\right) \qquad (10)$$

where $D_{k,\mathrm{aq}}$ is the diffusion coefficient and $\gamma_{k,\mathrm{aq}}$ the activity coefficient of ions k in the sample solution, and δ_aq is the thickness of the aqueous film. When combining Eqs. (6) and (10), we immediately have

$$a_{k,\mathrm{aq}} - a'_{k,\mathrm{aq}} = \left(x'_{k,\mathrm{m}} - x^0_{k,\mathrm{m}}\right)\Delta a_{k,\mathrm{ex}} \qquad (11)$$

$$\Delta a_{k,\mathrm{ex}}(t) = \frac{D_\mathrm{m}\delta_\mathrm{aq}}{D_{k,\mathrm{aq}}\delta_\mathrm{m}(t)}\gamma_{k,\mathrm{aq}}\frac{R_\mathrm{tot}}{z_k} = q_k\frac{d_\mathrm{m}}{\delta_\mathrm{m}(t)}\frac{R_\mathrm{tot}}{z_k} \qquad (12)$$

where $\Delta a_{k,\mathrm{ex}}$ is the highest possible deviation obtained between the bulk activity and the boundary activity of the sample, as resulting from the interfacial ion-exchange process. Evidently, this time-dependent activity increment depends on the ratio q_k between the ion permeability of the membrane phase and that of the aqueous diffusion layer [4], on the ratio between the total thickness d_m and the diffusion-layer thickness $\delta_\mathrm{m}(t)$ of the membrane, and on the ion-exchange capacity given by the total equivalent R_tot/z_k of ionic sites in the membrane. The maximum deviation between a_k and a'_k is obviously obtained for $x'_{k,\mathrm{m}} = 1$ and $x^0_{k,\mathrm{m}} = 0$, that is, when a membrane with zero initial concentration of ion k is exposed to a high sample activity of this ion.

When the boundary activity in Eq. (11) is substituted from Eq. (3), a solution for $x'_{k,\mathrm{m}}$ can be found

$$x'_{k,\mathrm{m}} = \frac{a_{k,\mathrm{aq}} + x^0_{k,\mathrm{m}}\Delta a_{k,\mathrm{ex}}}{\left(\frac{\Psi_i}{K_{ik}}\right)^{z_k/z_i} + \Delta a_{k,\mathrm{ex}}} \qquad (13)$$

which holds for any ion k (also for $k = i$ with $K_{ik} = 1$). The potential function Ψ_i, defined in Eq. (14), is finally determined from the general implicit solution in Eq. (15), which follows from Eqs. (13), (5) and (9):

$$E = E^0_i + \frac{RT}{z_i F}\ln\Psi_i \qquad (14)$$

$$\sum_k \frac{x^0_{k,\mathrm{m}}\left(\frac{\Psi_i}{K_{ik}}\right)^{z_k/z_i} - a_{k,\mathrm{aq}}}{\left(\frac{\Psi_i}{K_{ik}}\right)^{z_k/z_i} + \Delta a_{k,\mathrm{ex}}} = 0 \qquad (15)$$

This result is formally equivalent to a relationship that was derived earlier for the steady-state response of ISEs in the presence of different ions [4]. In the new approach, however, the parameters $\Delta a_{k,\mathrm{ex}}$ evidently vary with $t^{-1/2}$. A reduced expression can be derived for cases with only two ionic species i and j

$$\begin{aligned}\Psi_i^{1+z_j/z_i} &- \Psi_i^{z_j/z_i}\left(a_{i,\mathrm{aq}} - P_{ij}x^0_{j,\mathrm{m}}\Delta a_{j,\mathrm{ex}}\right) \\ &- \Psi_i K_{ij}^{z_j/z_i}\left(a_{j,\mathrm{aq}} - x^0_{i,\mathrm{m}}\Delta a_{j,\mathrm{ex}}\right) \\ &- K_{ij}^{z_j/z_i}\Delta a_{j,\mathrm{ex}}\left(a_{i,\mathrm{aq}} + P_{ij}a_{j,\mathrm{aq}}\right) = 0\end{aligned} \qquad (16)$$

$$P_{ij} = \frac{\Delta a_{i,\mathrm{ex}}}{\Delta a_{j,\mathrm{ex}}} = \frac{z_j D_{j,\mathrm{aq}}\gamma_{i,\mathrm{aq}}}{z_i D_{i,\mathrm{aq}}\gamma_{j,\mathrm{aq}}} \qquad (17)$$

$$\Delta a_{j,\mathrm{ex}}(t) = \frac{\gamma_{j,\mathrm{aq}}R_\mathrm{tot}\sqrt{D_\mathrm{m}}\delta_\mathrm{aq}}{z_j D_{j,\mathrm{aq}}\sqrt{2t}} \qquad (18)$$

where K_{ij} is the equilibrium selectivity coefficient, P_{ij} is a kinetic selectivity coefficient given by the ratio of ion permeabilities in the aqueous phase, and $\Delta a_{j,\mathrm{ex}}$ is the highest possible activity change for the ion j at the interface. P_{ij} is time-independent and usually approximates unity. An explicit solution is finally obtained when the two ions have the same charge $z_i = z_j = 1$

$$\begin{aligned}\Psi_i = 0.5\Big[\left(a_{i,\mathrm{aq}} + K_{ij}a_{j,\mathrm{aq}}\right) - \left(K_{ij}x^0_{i,\mathrm{m}} + P_{ij}x^0_{j,\mathrm{m}}\right)\Delta a_{j,\mathrm{ex}}\Big] \\ + \sqrt{0.25\left[\left(a_{i,\mathrm{aq}} + K_{ij}a_{j,\mathrm{aq}}\right) - \left(K_{ij}x^0_{i,\mathrm{m}} + P_{ij}x^0_{j,\mathrm{m}}\right)\Delta a_{j,\mathrm{ex}}\right]^2 + K_{ij}\Delta a_{j,\mathrm{ex}}\left(a_{i,\mathrm{aq}} + P_{ij}a_{j,\mathrm{aq}}\right)}\end{aligned} \qquad (19)$$

Similar results for steady-state cases were reported earlier [4,9,31,32]. Time-dependent responses according to Eq. (19) are discussed in the following.

3. Computer simulations

To demonstrate the applicability of the new theory, the response curves predicted by Eq. (19) were compared with results obtained from virtual experiments on ISEs. For such purposes, computer simulations based on finite-difference procedures were developed, as described in detail recently [23]. The ISE membrane, assumed to be 200 μm thick, was segmented into 19 internal elements of 10 μm thickness and two half-elements for the boundaries. The aqueous diffusion layer between membrane surface and sample was modelled by a total of six elements, of which the terminal one is counted as a half-element since the properties in its center are identical to those of the bulk solution. This made it possible to replace the differentials in the diffusion equations by finite differences between the centers of neighboring elements [23]. Accordingly, the evolution of concentration and potential profiles and of ion fluxes could easily be analyzed in the space and time domains, even for relatively complex cases. To this end, the flux-induced changes in the system were evaluated for typical time steps of 1 ms, starting from a given initial state. In the present study the ISE membrane was assumed to be prepared and preconditioned with primary ions only, that is, to be initially free from any interfering ions.

The same parameters were used for the calculations based on Eq. (19) and for the computer simulations. The exchangeable ions k in the ISE membrane were assumed to be singly charged, and to have a diffusion coefficient of $D_m = 10^{-8}\,cm^2\,s^{-1}$ and a total concentration of $R_{tot} = 0.01$ M. The thickness of the aqueous diffusion layer was taken as $\delta_{aq} = 55$ μm, which corresponds to experimental conditions with fast sample flow [23,29,30]. For simplicity, a common diffusion coefficient of $D_{k,aq} = 10^{-5}\ cm^2\ s^{-1}$ was chosen for all ions k, and the approximation $\gamma_{k,aq} = 1$ was used. Accordingly, the limiting selectivity coefficient in the flux-controlled domain was given by $P_{ij} = 1$.

4. Results and discussion

As a preliminary test, the computer simulation was applied for performing virtual experiments on ISEs in the absence of interfering ions j. In this case, the composition of the membrane remains constant, and mass transport is restricted to the aqueous diffusion layer. Fig. 1 documents the emf vs. time response obtained for a 10-fold increase and decrease in the activity of the primary ion i, respectively. The results of these virtual experiments are found to be in excellent agreement with curves calculated from the Markovic–Osburn theory of purely diffusion-controlled activity changes at the electrode surface [24,33,34]. The standard deviation between simulated points and exact curves is only ±0.1 mV. This clearly shows that numerical simulations are a powerful method for ISE studies, even when the analysis involves only a small number of finite elements (see also [23]). The data in Fig. 1 also indicate that diffusion through the 55-μm-thick unstirred layer is completed within a few seconds. Hence, the theoretical description given in Section 2 can be applied as a good approximation without the need for any time corrections resulting from this diffusion-time delay.

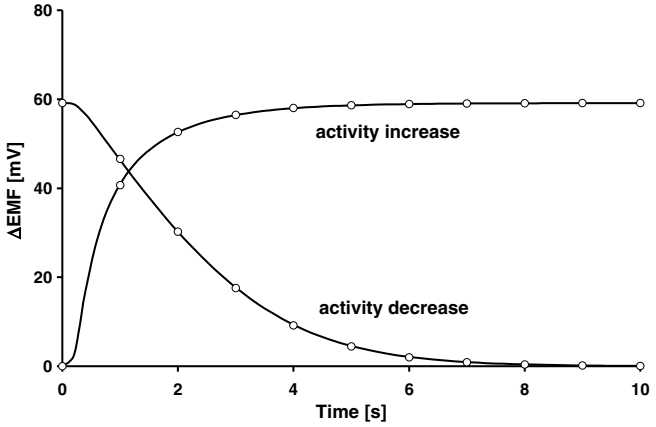

Fig. 1. EMF-time response of an ISE to a 10-fold increase or decrease in the activity of primary ions. The ion flux through the aqueous diffusion layer on the ISE was analyzed using a diffusion coefficient of $D_{i,aq} = 10^{-5}\,cm^2\,s^{-1}$ and a diffusion layer thickness of $\delta_{aq} = 0.0055$ cm. Data points obtained from the computer simulation are compared with curves predicted from the exact theory [24,33,34].

The time-dependent selectivity behavior of ISEs is investigated extensively in the following. For this purpose, potential responses to different interfering ions j were calculated from Eqs. (14) and (19) and compared with the results of virtual experiments by computer simulation. It was a basic assumption concerning the experimental procedure that the ISE membrane was prepared and preconditioned with primary ions i only. This idealized electrode was assumed to be available for each separate measurement. At the time $t = 0$, the ISE was exposed to the sample solution containing an interfering ion j, and the emf values were recorded as a function of t. The response data after well-defined measuring periods were finally evaluated, which guarantees for an unbiased comparison of selectivity patterns. This is in contrast to conventional experiments where a complete series of measurements on different samples is carried out with the same ISE, without an intermediate reconditioning or even replacement of the membrane. Virtual experiments conforming to the latter conditions were described earlier [23].

Fig. 2 shows calibration plots for several interfering ions j that are preferred by the ISE over the primary ion ($K_{ij} \gg 1$) but differ in the thermodynamically defined selectivity coefficient K_{ij}. The studied selectivity measurements conform to the fixed-primary-ion method since a constant 0.1 M background of ions i was added to the sample solutions. The emf values obtained from the computer simulations for measuring periods of 2.5 min are compared with theoretical curves plotted according to Eqs. (14) and (19). Evidently, the theory is well capable of fitting the results of the virtual experiments for all examples. The ISE system with $K_{ij} = 10^6$ exhibits a super-nernstian response region

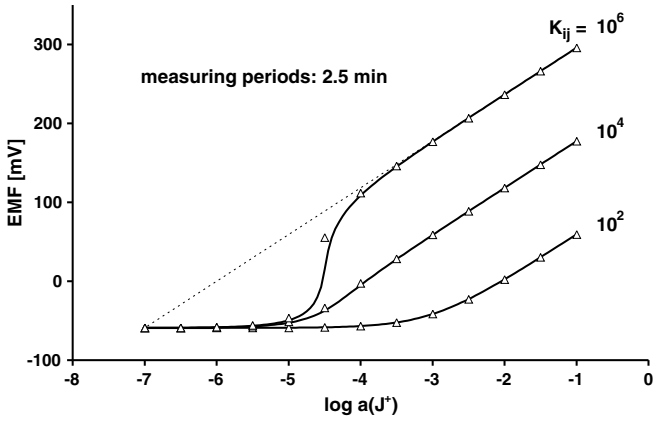

Fig. 2. EMF response of an ISE to solutions of interfering ions with $K_{ij} = 10^2$, 10^4, and 10^6, respectively, after constant measuring periods of 2.5 min. The samples also contained a 0.1 M background of primary ions. The points represent data from virtual experiments based on computer simulations. The curves are results from calculations according to Eqs. (14) and (19). The dotted line shows the nernstian response for $K_{ij} = 10^6$. The same parameters were used for all examples (see Section 3).

centered at $10^{-4.5}$ M, which documents the transition between the nearly thermodynamical selectivity characteristics at $>10^{-4}$ M and the simply permeability-controlled non-selective behavior at $<10^{-5}$ M [4,9,12,35]. The exact position of the super-nernstian response region mainly depends on the membrane parameters and can be drastically shifted for ISE configurations with built-in ion fluxes [26] (see also Appendix). Detailed explanations using schematics that illustrate the underlying ion-flux influences have been presented earlier [2–4]. Analogous phenomena are expected for the other two systems in Fig. 2, but the effects are here hidden because the samples contain high levels of primary ions. Measurements on pure solutions of interfering ions are reported later.

Fig. 3 summarizes results of selectivity studies that were performed on the ISE system with $K_{ij} = 10^6$ by using different measuring periods. Both the virtual experiments and the theoretical plots demonstrate that the range with near-equilibrium selectivity behavior can be extended to lower activities by simply increasing the measuring time per sample. Thus, an increase from 2.5 to 10 min results in a shift of the super-nernstian region of almost one decade on the activity scale. This is also documented in Fig. 4 where calibration curves for measuring periods of 0.625–160 min are presented. It is expected that the achievable effects would even be magnified when the measurements on the samples from 0.1 M to 10^{-8} M are made in one series, using the same ISE without any reconditioning. Then the total time period during which the membrane is exposed to solutions of the interfering ion increases from sample to sample. Virtual experiments of this kind were reported earlier and were found to yield hysteresis phenomena depending on the direction of activity changes [23]. It has to be pointed out that the time-dependent effects shown in Fig. 4 are in good agreement with results obtained in real experiments [22].

Additional results on the time-dependent selectivity characteristics of ISEs are presented in Fig. 5. It illustrates the potential changes as a function of t after the replacement of an initial solution of ions i by an equimolar pure solution of the species j. Such time responses are given for three systems that would exhibit an equilibrium selectivity of $K_{ij} = 10$, 10^2, and 10^3, respectively. These selectivity values are obviously established within a short time period if the sample activities are sufficiently high. On the other hand, the measurements on the 10^{-5} M samples are found to be far from the equilibrium response. In the early stage, the small emf changes actually suggest an apparent selectivity coefficient of about unity. In Fig. 5 the data obtained from the computer simulations are again compared with curves calculated from the new theory. The theory is evidently capable of nicely reconstructing the data points, although the agreement is not perfect. The plotted

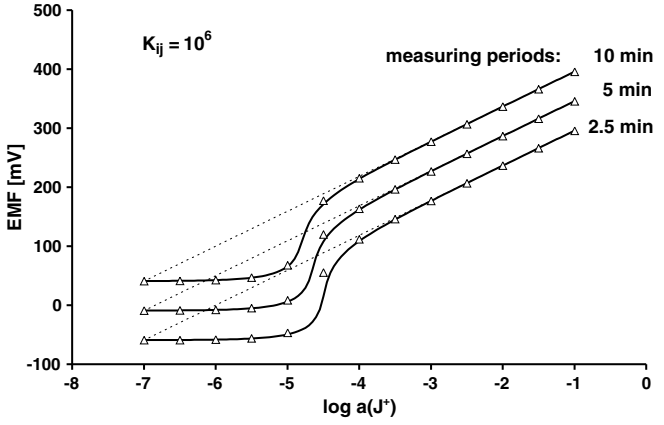

Fig. 3. EMF response to interfering ions with $K_{ij} = 10^6$ after measuring periods of 2.5, 5, and 10 min, respectively. Data points from computer simulations are compared with theoretical curves (for more details see Fig. 2). The responses after 5 and 10 min were arbitrarily shifted by 50 and 100 mV, respectively.

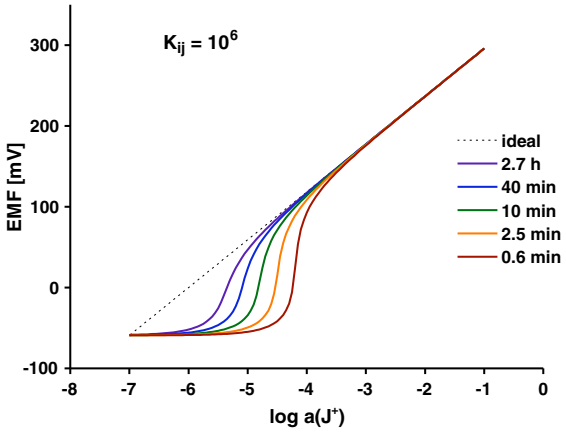

Fig. 4. Calculated response curves from Eqs. (14) and (19) for interfering ions with $K_{ij} = 10^6$ after measuring periods of $\Delta t = 0.625$, 2.5, 10, 40, and 160 min, respectively. The total time of exposure of the ISE to interfering ions was Δt for each sample. The dotted line shows the nernstian response for $K_{ij} = 10^6$.

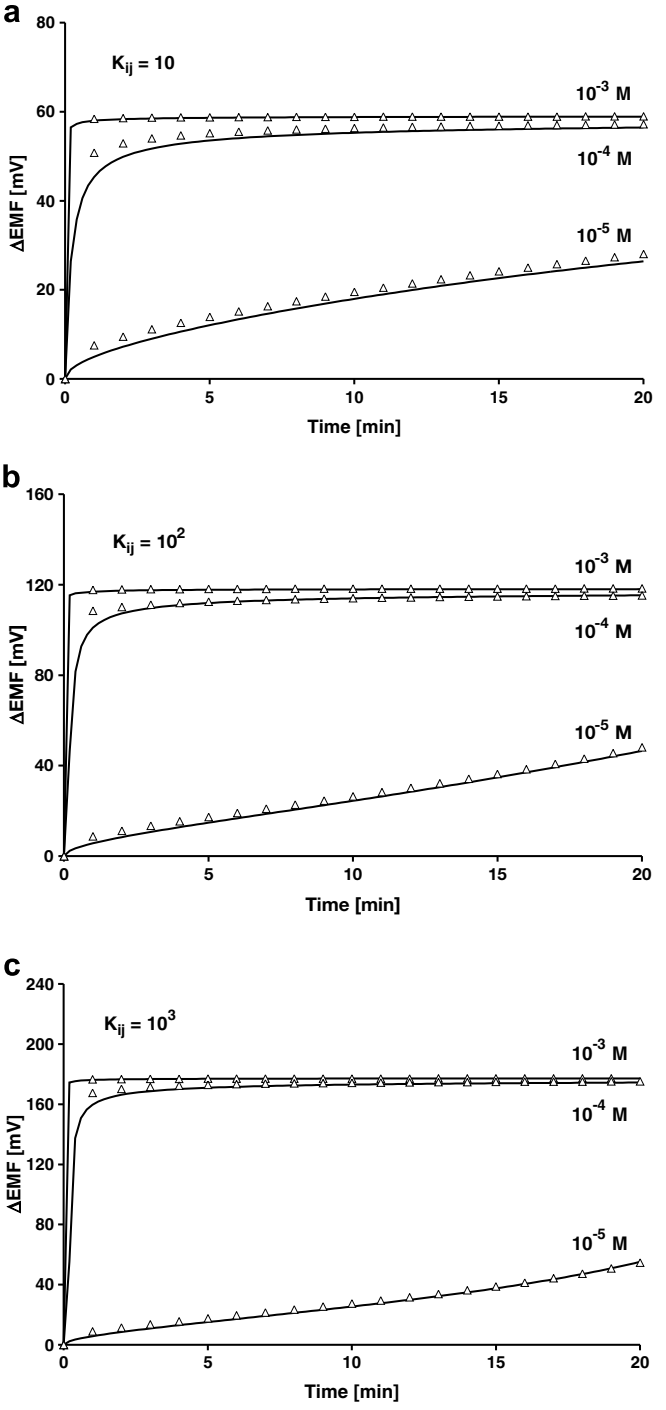

Fig. 5. EMF-time response after the replacement of primary ion solutions by equimolar pure solutions of interfering ions. ISE systems with $K_{ij} = 10$ (a), 10^2 (b), and 10^3 (c) were exposed to sample activities of 10^{-3}, 10^{-4}, and 10^{-5} M, respectively. Data points from computer simulations are compared with theoretical curves.

curves reflect many details of the virtual experiments as for instance the late steeper potential increase found for one curve in Fig. 5c.

Fig. 6 shows calibration curves for ions j with $K_{ij} \ll 1$, as determined in measurements of 2.5 min duration. The case with $K_{ij} = 1$, which can be identified with the primary-ion response, is also included. For ions that are discriminated

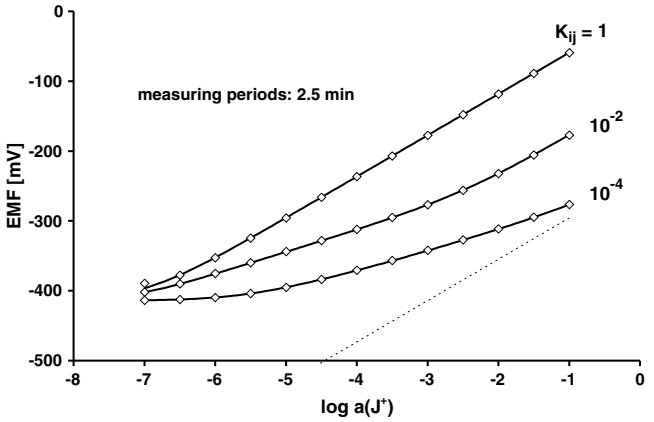

Fig. 6. EMF response to interfering ions with $K_{ij} = 1$, 10^{-2}, and 10^{-4}, respectively, after constant measuring periods of 2.5 min. The samples also contained a 10^{-7} M background of primary ions. Data points from computer simulations are compared with theoretical curves (for details see Fig. 2). The response for $K_{ij} = 1$ is equivalent to the primary-ion response. The dotted line shows the nernstian response for $K_{ij} = 10^{-4}$.

by the ISE, the transition between the equilibrium and the kinetic domains of ion selectivity obviously occurs in a broad activity range where the slopes of the response curves are reduced to about half of the nernstian slope (see also [4,9,35]). This fact is evident from both the virtual experiments and the theoretical plots, which attest an excellent agreement. The sub-nernstian responses are in clear contrast to the ones found in Figs. 2–4 for $K_{ij} \gg 1$. The present results for $K_{ij} \ll 1$ document that selectivity coefficients near the hypothetical equilibrium values can be realized only at the highest sample activities. At lower activities, the selectivity behavior is usually far from the thermodynamically controlled domain, unless the studied ISE membrane has initially not been prepared with the respective interfering ion j instead of the primary ion i [36]. This holds at least for relatively short measurements. The calculated curves in Fig. 7 illustrate that an enormous

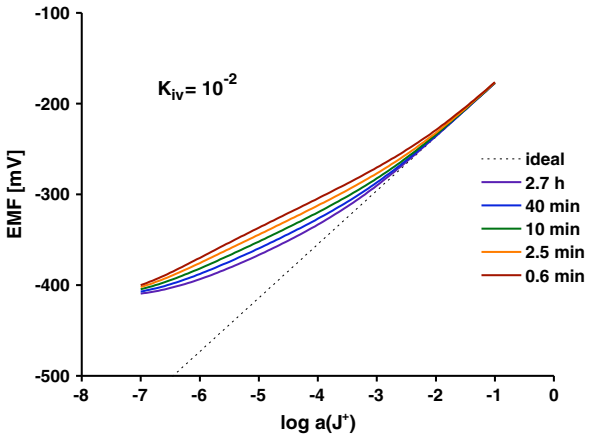

Fig. 7. Calculated response curves for interfering ions with $K_{ij} = 10^{-2}$ after measuring periods of $\Delta t = 0.625$, 2.5, 10, 40, and 160 min, respectively. The samples contained a 10^{-7} M background of primary ions. Otherwise, the conditions are the same as in Fig. 4. The dotted line shows the nernstian response for $K_{ij} = 10^{-2}$.

increase of the measuring periods would be needed for really improving the selectivity characteristics at lower activities. As a matter of fact, the influence of the measuring time on the response curves is here much less pronounced than in Fig. 4. It should also be noted that a final steady state is generally reached when the diffusion-layer thickness $\delta_m(t)$ approaches the total membrane thickness d_m. In this case the present theory is still applicable after insertion of the steady-state condition $\delta_m(t) = d_m$ in Eq. (12).

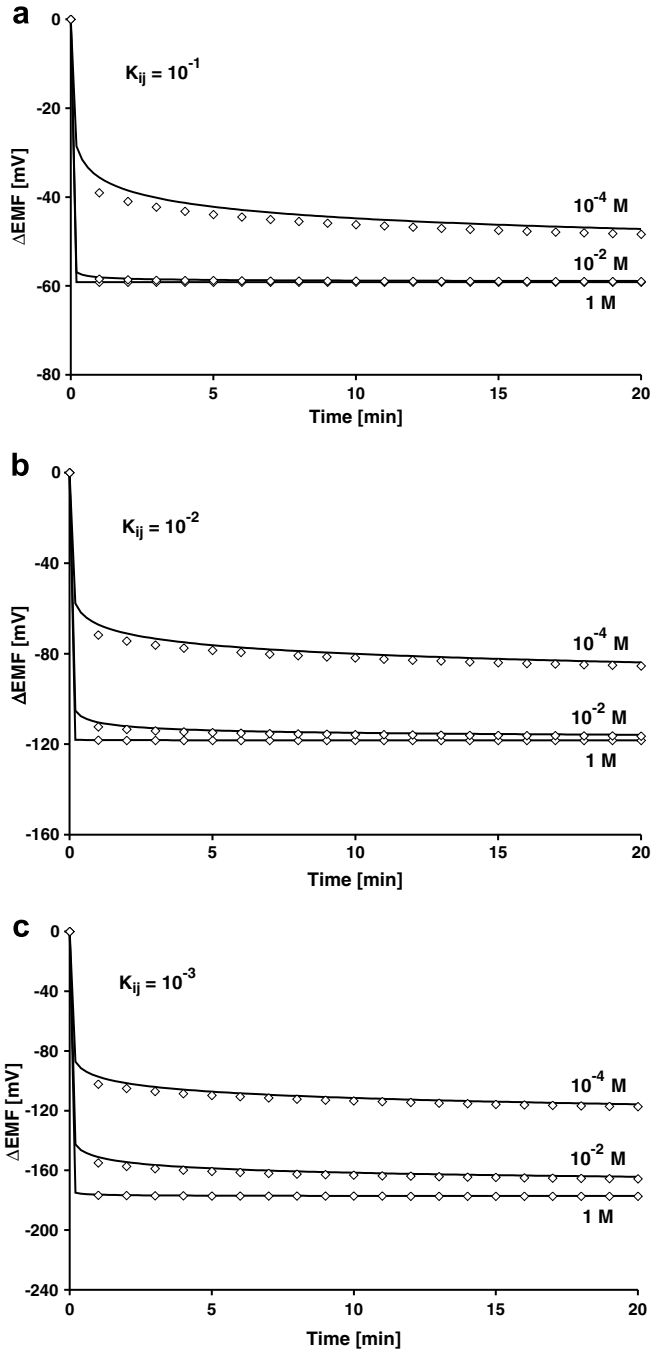

Fig. 8. EMF–time response after the replacement of primary ion solutions by equimolar pure solutions of interfering ions. ISE systems with $K_{ij} = 10^{-1}$ (a), 10^{-2} (b), and 10^{-3} (c) were exposed to sample activities of 1, 10^{-2}, and 10^{-4} M, respectively. Data points from computer simulations are compared with theoretical curves.

Fig. 8 shows the potential vs. time response of ISEs to pure solutions of interfering j ions with $K_{ij} \ll 1$. These selectivity studies are analogous to the ones given before in Fig. 5. Evidently, the present systems soon reach the equilibrium response with a selectivity of $K_{ij} = 10^{-1}$, 10^{-2}, and 10^{-3}, respectively, if the sample activity is as high as 1 M. For 10^{-2} M and especially for 10^{-4} M solutions, the equilibration process is much slower and mimics an apparent selectivity coefficient that is intermediate between the real K_{ij} and unity. The simulated responses in Fig. 8 are again compared with theoretical curves. The results attest a good agreement between the theoretical curves and the data points.

5. Conclusions

A theoretical description of the time-dependent potential response of ISEs to sample solutions that contain primary and interfering ions was presented. The theory permits it to approximately predict the variations in the apparent ion-selectivity behavior as expected with increasing measuring time. To demonstrate the applicability of the theory, calculated response curves were compared with the results of virtual experiments based on computer simulations. A close and convincing agreement was achieved for a large series of different examples. An average standard deviation of about 2 mV was realized in these studies, which is fairly low in comparison with the whole covered potential range of 700 mV. The results suggest that the new theory can be successfully applied for general cases. The present study confirms that nearly unbiased selectivity coefficients can be determined only by relatively long measurements at sufficiently high activities of the studied ions.

Appendix. Extension of the theory for membranes with asymmetrical preconditioning modes

The treatment in Section 2 is restricted to membranes that initially have a uniform ionic composition. In practice, however, ISEs are often preconditioned with different aqueous solutions on both sides of the membrane. Hence the initial molar fractions $x^0_{k,m}$ of ions k on the membrane surface exposed to the sample side will differ from the molar fractions $x^*_{k,m}$ on the inner surface. Accordingly, diffusion fluxes are also present in the initial steady state and have to be considered as additional terms in the respective Eq. (6)

$$J_k = \frac{D_m}{\delta_m(t)}\left(x'_{k,m} - x^0_{k,m}\right)R_{tot}/z_k + \frac{D_m}{d_m}\left(x^0_{k,m} - x^*_{k,m}\right)R_{tot}/z_k \quad \text{(A.1)}$$

where d_m is the total membrane thickness, and $\delta_m(t) \leqslant d_m$ is the diffusion-layer thickness at the time t, as induced

by the sample change at $t = 0$. We then obtain an extended version of Eq. (11)

$$a_{k,\mathrm{aq}} - a'_{k,\mathrm{aq}} = \left(x'_{k,\mathrm{m}} - x^0_{k,\mathrm{m}}\right)\Delta a_{k,\mathrm{ex}} + \left(x^0_{k,\mathrm{m}} - x^*_{k,\mathrm{m}}\right)\Delta a^{\mathrm{st}}_{k,\mathrm{ex}} \quad (A.2)$$

where $\Delta a_{k,\mathrm{ex}}$ is the time-dependent activity increment defined in Eq. (12), and $\Delta a^{\mathrm{st}}_{k,\mathrm{ex}}$ is the corresponding value for the steady state, that is for $\delta_{\mathrm{m}}(t) = d_{\mathrm{m}}$

$$\Delta a^{\mathrm{st}}_{k,\mathrm{ex}} = \frac{D_{\mathrm{m}}\delta_{\mathrm{aq}}}{D_{k,\mathrm{aq}}d_{\mathrm{m}}}\gamma_{k,\mathrm{aq}}\frac{R_{\mathrm{tot}}}{z_k} = q_k\frac{R_{\mathrm{tot}}}{z_k} \quad (A.3)$$

Eq. (A.2) can be combined with Eq. (3) to yield a generalized description of the potential response. The respective result for systems with two ions i and j of the same charge is finally given by

$$\Psi_i = 0.5\left[\left(a_{i,\mathrm{aq}} + K_{ij}a_{j,\mathrm{aq}}\right) - \Delta a_{\mathrm{tot}}\right] + \sqrt{0.25\left[\left(a_{i,\mathrm{aq}} + K_{ij}a_{j,\mathrm{aq}}\right) - \Delta a_{\mathrm{tot}}\right]^2 + K_{ij}\Delta a_{j,\mathrm{ex}}\left(a_{i,\mathrm{aq}} + P_{ij}a_{j,\mathrm{aq}}\right)} \quad (A.4)$$

$$\Delta a_{\mathrm{tot}} = \left(K_{ij}x^0_{i,\mathrm{m}} + P_{ij}x^0_{j,\mathrm{m}}\right)\left(\Delta a_{j,\mathrm{ex}} - \Delta a^{\mathrm{st}}_{j,\mathrm{ex}}\right) + \left(K_{ij}x^*_{i,\mathrm{m}} + P_{ij}x^*_{j,\mathrm{m}}\right)\Delta a^{\mathrm{st}}_{j,\mathrm{ex}} \quad (A.5)$$

which differs from Eq. (19) in the definition of the overall activity increment Δa_{tot}. Eq. (A.4) reduces to the former result for short times when it holds that $\Delta a_{j,\mathrm{ex}} \gg \Delta a^{\mathrm{st}}_{j,\mathrm{ex}}$. The final steady-state behavior for $\Delta a_{j,\mathrm{ex}} = \Delta a^{\mathrm{st}}_{j,\mathrm{ex}}$ is described by an analogous expression where, however, the ionic composition at the inner membrane boundary becomes decisive for Δa_{tot}. Accordingly, the apparent selectivity behavior after short periods depends on the preconditioning solution on the sample side (influence of $x^0_{i,\mathrm{m}}$ and $x^0_{j,\mathrm{m}}$), whereas the long-term selectivity more depends on the inner solution (influence of $x^*_{i,\mathrm{m}}$ and $x^*_{j,\mathrm{m}}$).

Appropriate solution of the diffusion equations

An explicit solution of the diffusion equations for a two-phase system with current-coupled ion fluxes and non-linear interfacial distribution relationships is not available. However, useful descriptions can be found for some special cases.

Case I: This is the example of an ISE membrane containing primary ions that is exposed to a relatively concentrated solution of interfering ions with $K_{ij} \gg 1$. Since the original ions i at the membrane surface are rapidly replaced by the new species j, we can use the boundary conditions $C'_{j,\mathrm{m}} = C^0_{j,\mathrm{m}} = 0$ for $t < 0$ and $C'_{j,\mathrm{m}} = R_{\mathrm{tot}}$ for $t \geqslant 0$ as a good approximation. The corresponding solution of the diffusion equations leads to Eq. (A.1) for the flux of ions j into the membrane [27]

$$J_j = \frac{D_{\mathrm{m}}C'_{j,\mathrm{m}}}{\sqrt{\kappa_1 D_{\mathrm{m}}t}} \quad \text{with } \kappa_1 = \pi \quad (A.6)$$

where the symbols are the same as in Section 2, and where κ_1 turns out to be the highest possible value of κ. Eq. (A.6) is analogous to the result for the time-dependent diffusion flux in the aqueous phase from or to a conventional metal electrode during a chronoamperometric experiment [28].

Case II: In this case, the ISE membrane with primary ions is exposed to a highly diluted solution of interfering ions with $K_{ij} \gg 1$. Here, the ion exchange at membrane surface drastically reduces the interfacial activity of ions j. Hence, from Eq. (10) with $a'_{j,\mathrm{aq}} = 0$, we obtain the boundary condition $J_j = \mathrm{const}(t)$, which is valid at least for a short time period. The corresponding solution for the boundary concentration is $C'_{j,m} = 2J_j\sqrt{(t/\pi D_m)}$ [27]. An analogous expression applies to the aqueous boundary concentration at the surface of a metal electrode at constant electrolysis current in a chronopotentiometric experiment [28]. Finally, this leads to the relationship

$$J_j = \frac{D_{\mathrm{m}}C'_{j,\mathrm{m}}}{\sqrt{\kappa_2 D_{\mathrm{m}}t}} \quad \text{with } \kappa_2 = 4/\pi \quad (A.7)$$

where κ_2 can be considered as the minimal value of κ.

For more general cases, an intermediate situation between the above limiting cases I and II may be encountered. It is therefore reasonable and appropriate to use the geometrical mean of κ_1 and κ_2 as a common representative value for all virtual experiments

$$\kappa = \sqrt{\kappa_1\kappa_2} = 2 \quad (A.8)$$

This permits it to approximate the diffusion fluxes and the resulting effects on the ISE response for a wide range of experimental conditions.

References

[1] J. Koryta, K. Stulik, Ion-Selective Electrodes, Cambridge University Press, Cambridge, GB, 1983.
[2] T. Sokalski, T. Zwickl, E. Bakker, E. Pretsch, Anal. Chem. 71 (1999) 1204.
[3] T. Sokalski, A. Ceresa, M. Fibbioli, T. Zwickl, E. Bakker, E. Pretsch, Anal. Chem. 71 (1999) 1210.
[4] W.E. Morf, M. Badertscher, T. Zwickl, N.F. de Rooij, E. Pretsch, J. Phys. Chem. B 103 (1999) 11346.
[5] A. Ceresa, A. Radu, S. Peper, E. Bakker, E. Pretsch, Anal. Chem. 74 (2002) 4027.
[6] E. Bakker, E. Pretsch, Trends Anal. Chem. 24 (2005) 199.
[7] E. Bakker, E. Pretsch, Angew. Chem., Int. Ed. Engl. 46 (2007) 5660.

[8] Z. Szigeti, T. Vigassy, E. Bakker, E. Pretsch, Electroanalysis 18 (2006) 1254.
[9] W.E. Morf, The Principles of Ion-Selective Electrodes and of Membrane Transport, Elsevier, New York, 1981.
[10] E. Bakker, E. Pretsch, P. Bühlmann, Anal. Chem. 72 (2000) 1127.
[11] M.E. Meyerhoff, B. Fu, E. Bakker, J.H. Yun, V.C. Yang, Anal. Chem. 68 (1996) 168A.
[12] T. Vigassy, W.E. Morf, M. Badertscher, A. Ceresa, N.F. de Rooij, E. Pretsch, Sens. Actuat. B 76 (2001) 477.
[13] S. Makarychev-Mikhailov, A. Shvarev, E. Bakker, J. Am. Chem. Soc. 126 (2004) 10548.
[14] S. Peper, A. Ceresa, E. Bakker, E. Pretsch, Anal. Chem. 73 (2001) 3768.
[15] K. Tompa, K. Birbaum, A. Malon, T. Vigassy, E. Bakker, E. Pretsch, Anal. Chem. 77 (2005) 7801.
[16] A. Malon, E. Bakker, E. Pretsch, Anal. Chem. 79 (2007) 632.
[17] E. Lindner, R.E. Gyurcsányi, R.P. Buck, Electroanalysis 11 (1999) 695.
[18] E. Pergel, R.E. Gyurcsányi, K. Tóth, E. Lindner, Anal. Chem. 73 (2001) 4249.
[19] W.E. Morf, M. Badertscher, T. Zwickl, N.F. de Rooij, E. Pretsch, J. Electroanal. Chem. 526 (2002) 19.
[20] A. Shvarev, E. Bakker, Anal. Chem. 75 (2003) 4541.
[21] T. Sokalski, P. Lingenfelter, A. Lewenstam, J. Phys. Chem. B 107 (2003) 2443.
[22] P. Lingenfelter, I. Bedlechowicz-Sliwakowska, T. Sokalski, M. Maj-Zurawska, A. Lewenstam, Anal. Chem. 78 (2006) 6783.
[23] W.E. Morf, E. Pretsch, N.F. de Rooij, J. Electroanal. Chem. 602 (2007) 43.
[24] W.E. Morf, W. Simon, in: H. Freiser (Ed.), Ion-Selective Electrodes in Analytical Chemistry, Plenum Press, New York, 1978.
[25] G.G. Guilbault, R.A. Durst, M.S. Frant, H. Freiser, E.H. Hansen, T.S. Light, E. Pungor, G. Rechnitz, N.M. Rice, T.J. Rohm, W. Simon, J.D.R. Thomas, Pure Appl. Chem. 48 (1976) 127.
[26] A. Radu, A.J. Meir, E. Bakker, Anal. Chem. 76 (2004) 6402.
[27] J. Crank, The Mathematics of Diffusion, Oxford University Press, New York, 1993.
[28] A.J. Bard, L.R. Faulkner, Electrochemical Methods, Wiley, New York, 2001.
[29] G. Kortüm, Lehrbuch der Elektrochemie, Verlag Chemie, Weinheim, 1972.
[30] W. Kemula, W. Kutner, in: E. Pungor (Ed.), Modern Trends in Analytical Chemistry, Akadémiai Kiado, Budapest, 1984, p. 3.
[31] W.E. Morf, in: E. Pungor (Ed.), Ion-Selective Electrodes 3, Akadémiai Kiadó, Budapest, 1981.
[32] J. Senkyr, J. Petr, in: E. Pungor (Ed.), Ion-Selective Electrodes 3, Akadémiai Kiadó, Budapest, 1981.
[33] W.E. Morf, E. Lindner, W. Simon, Anal. Chem. 47 (1975) 1596.
[34] P.L. Markovic, J.O. Osburn, AIChE J. 19 (1973) 504.
[35] A. Hulanicki, R. Lewandowski, Chem. Anal. (Warsaw) 19 (1974) 53.
[36] E. Bakker, Anal. Chem. 69 (1997) 1061.